Journal of Luminescence 211 (2019) 203–208

Contents lists available at ScienceDirect

Journal of Luminescence

journal homepage: www.elsevier.com/locate/jlumin

Full Length Article

Size effects and radiation resistance of BaF_2 nanophosphors

O.T. Antonyak[a,*], V.V. Vistovskyy[a], A.V. Zhyshkovych[a], I.M. Kravchuk[b]

[a] Ivan Franko National University of Lviv, 8 Kyrylai Mefodiya Street, 79005, Lviv, Ukraine
[b] Lviv Polytechnic National University, 12 S. Bandery Street, 79000, Lviv, Ukraine

ARTICLE INFO

Keywords:
BaF_2 nanoparticles
X-ray excited luminescence spectra
Thermally stimulated luminescence
Size effects
Radiation resistance

ABSTRACT

The stationary X-ray excited luminescence (XEL) spectra at 80 and 294 K as well as the thermally stimulated luminescence (TSL) in the 80–300 K range of a single crystal and nanoparticles of BaF_2 with various grain sizes of 20–113 nm were studied. Under the influence of size effects in BaF_2 nanophosphors, a short-wave displacement of self-trapped excitons emission band was observed compared to the corresponding single crystal, and its splitting into two components peaked at 324 and 305 nm for 294 K, and at 321 and 305 nm – for 80 K.

A slight decrease of radiation resistance of BaF_2 nanophosphors was observed in comparison to single crystal, which led to additional band of X-ray excited luminescence at ~410 nm that may be associated with emission of exciton localized in the vicinity of anionic vacancies of the matrix. At the same time, it was established that radiation resistance of BaF_2 nanophosphors is much higher compared to the corresponding CaF_2 nanophosphors.

With the use of integral TSL curves and TSL spectra, it has been shown that V_H-centers with delocalization temperature of ~140 K are the main hole centers that occur in BaF_2 nanoparticles under X-ray irradiation influence, while in BaF_2 single crystals – these are V_k - and H-centers with delocalization temperatures at 113 and 198 K, respectively. Significant long-wave displacement of emission bands associated with (V_H-F)- and (H-F)-recombinations, compared to the spectra of corresponding single crystal, was observed in BaF_2 nanophosphors.

1. Introduction

In the recent years, there has been observed a clear tendency was observed to move from bulk scintillators and phosphors of a certain chemical composition to their nanocrystalline analogues [1–3]. Therefore it possible, in a number of cases, due to the effects of quantum confinement in nanoparticles [4,5], to improve some of important spectral and kinetic characteristics of appropriate detectors of ionization radiation, in particular, to reduce their decay time, and at the same time, to simplify and to cheapen technological production processes of scintillators and phosphors.

On the other hand, requirements for detection of high-energy quanta, in particular γ- and X-quanta, are related to stability problem of radiation indicators, which is well studied for bulk crystals, in particular, for alkaline earth halide crystals [6–10], but this is definitely insufficient for corresponding nanoparticle phosphors. At the same time, formation of radiation defects under of stationary irradiation influence by high-energy quanta may be quite peculiar in nanoparticles compared with bulk phosphors and should depend on both chemical composition and nanoparticle size. Radiation defect formation, in turn, can significantly change spectral-kinetic characteristics of nanophosphors. Namely, while measuring spectra of stationary X-ray excited luminescence in CaF_2 nanoparticles, in Ref. [11] there was revealed a series of intensive emission bands of excitons localized in the vicinity of radiation defects formed during irradiation of nanoparticles by stationary X-ray excitation, whereas during pulsed X-ray excitation of these nanoparticles, only one characteristic band of emission of self-trapped excitons in CaF_2 was detected at ~ 300 nm, which was previously found in Refs. [2,6]. Thus, a low radiation resistance of the CaF_2 nanoparticles was established during stationary X-ray quanta irradiation.

The subject of present study is investigation of size effects and radiation resistance of BaF_2 undoped nanophosphors by stationary X-irradiation. BaF_2 single crystal is known to be one of the most common scintillators for γ- and X-quanta with a record low decay time (τ = 0.6–0.8 ns) in the spectral region of 180–200 nm [1] that corresponds to high-speed core-valence transitions in BaF_2 matrix originally interpreted in Ref. [12]. However, light output of luminescence of BaF_2 crystals in this spectral region is rather low (just no more than 1500 photons/MeV). BaF_2 crystals also have a more intense inertial emission component (τ ~ 600 ns) at ~ 300 nm due to the self-trapped excitons (STE) [6,8]. Due to STE energy transfer to the corresponding activator ions in these crystals, it is possible to obtain phosphors and scintillators that emit in the longer-wave spectral regions (for example BaF_2:

---

[*] Corresponding author.
E-mail address: o.antonyak@gmail.com (O.T. Antonyak).

https://doi.org/10.1016/j.jlumin.2019.03.046
Received 27 December 2018; Received in revised form 22 March 2019; Accepted 23 March 2019

Ce^{3+} [6,8,13], BaF_2: Eu [6,14]).

Low-temperature, non-emitting STE decay in BaF_2 crystals can lead to the stable electron and hole color centers formation [7,9] which can be caused by their low radiation resistance, although it is known that probability of stable color centers formation in alkaline-earth fluorides crystals is much lower (0.001%) than in alkaline halide crystals (10%) [9].

In this paper, we compare stationary X-ray excited luminescence spectra of a single BaF_2 crystal in 280–600 nm range with corresponding spectra of nanoparticles of different sizes, as well as their thermostimulated luminescence in 80–300 K temperature range in order to assess the size factor effect on radiation resistance of BaF_2 nanoparticles.

2. Experiment

BaF_2 nanoparticles were synthesized by a low-temperature chemical method, using the procedure described in Ref. [2]. Then, nanophosphors were annealed in air at 200, 400, 600 and 800 C in order to increase the size of nanoparticles. Nanoparticle sizes were determined by X-ray diffraction using a STOE STADI P diffractometer [2], estimating diffraction peak width and using Sherer equation (Fig. 1).

The BaF_2 single crystal was grown using Stepanov–Stokbarger method. A sample for measuring having sizes of about 9.0 × 8.0 × 3.0 mm and cleaved of a solid single crystalline boule in parallel with cleavage plane {111}, was completely transparent and optically homogeneous.

Stationary X-ray excited luminescence spectra recorded with the use of a standard commercial X-ray source of the URS-55 type (Mo- anticathode, U = 40 kV, I = 10 mA) as well as TSL spectra were measured using equipment mounted on the base of mirror monochromator of the ZMR-3 type.

Prior to integral TSL curves and TSL spectra measurements, samples were irradiated at 80 K for 10 min using a URS-55 source. Heating of samples was carried out at a rate of 3.5 K/min.

3. Results and discussion

3.1. Stationary X-ray excited luminescence of single crystal and nanophosphors of BaF_2

At 294 and 80 K, the stationary X-ray excited luminescence spectra of the BaF_2 single crystal (Fig. 3, curves 1, 2) and of the corresponding nanoparticles of the size d = 78 ± 5 nm (T_a = 600 C) (Fig. 3, curves 3, 4) were investigated for which there was traced a maximum light emission for the BaF_2 nanoparticles studied.

The X-ray excited luminescence spectrum of a BaF_2 single crystal at 294 K contains one elementary Gaussian band with the half-width ΔE = 1.21 eV peaked at λ_m = 334 nm (Fig. 3, curve 1). The cooling of the sample to 80 K leads to a shift of this XEL peak to λ_m = 315 nm, reducing its half-width to ΔE = 0.93 eV and increasing its intensity by ~1.3 times. Simultaneously, during the cooling there occurs a weak additional long-wavelength component of the spectrum of λ_m ~410 nm and a half-width of ΔE = 0.61 eV. The nature of the temperature dependence and the spectral placement of the main radiation component of the BaF_2 single crystal allows it to be attributed to the previously studied STE emission in BaF_2 [6,8].

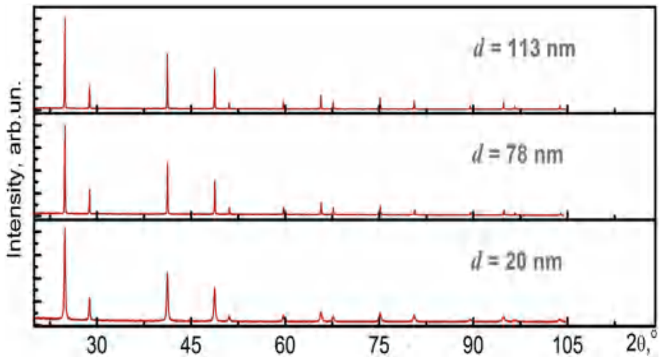

Fig. 1. Comparison of diffractograms of BaF_2 nanoparticles of different sizes. The dependence of nanoparticle average size d on annealing temperature is shown in Fig. 2.

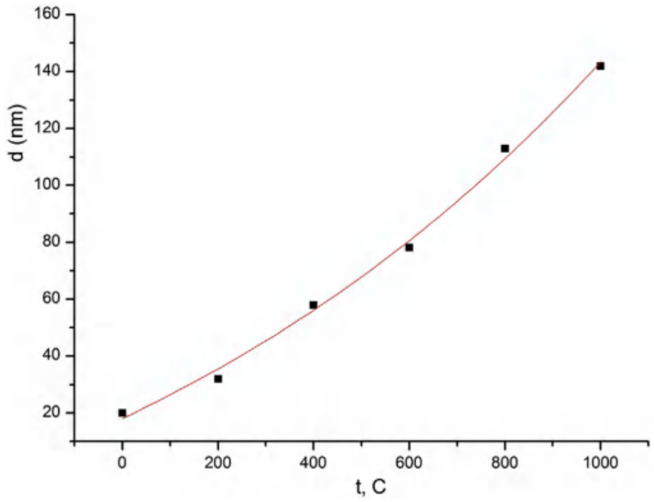

Fig. 2. Dependence of BaF_2 nanoparticle size d on annealing temperature t, C.

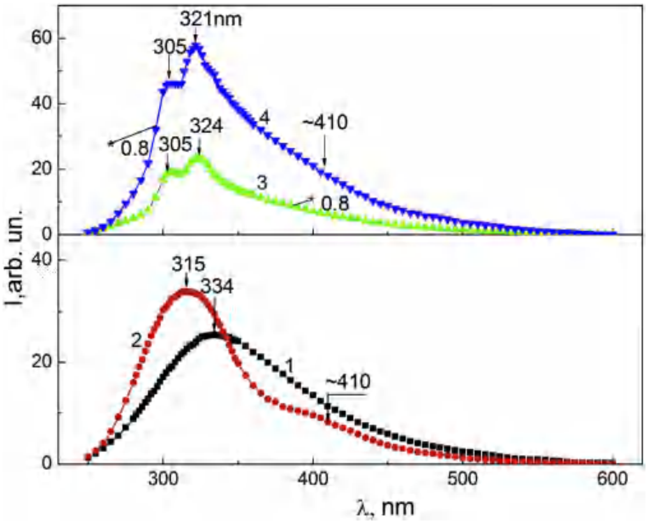

Fig. 3. X-ray excited luminescence spectra of the single crystal (1, 2) and the nanoparticles of BaF_2 with a grain size of 78 nm (3, 4): 1, 3–T = 294 K; 2, 4–T = 80 K.

The additional low-temperature XEL band of a single BaF_2 crystal at ~410 nm may belong to the emission of the exciton localized on the radiation defects of the matrix. It has been previously established [7] that during X-irradiation at 77 K of BaF_2 crystals, there appear stable radiation defect pairs in the form of V_k and F centers. It is well known that the F-center is an anionic vacancy that captures an electron. Thus, an additional XEL band of BaF_2 crystal at ~410 nm can correspond to the emission of the exciton localized in the vicinity of the anionic vacancy.

The spectra of X-ray excited luminescence of BaF_2 nanoparticles contain significant differences in comparison with the spectra of a single crystal. Specifically, for 294 K in the emission spectrum of BaF_2 nanoparticles with a grain size d = 78 ± 5 nm, there is a significant short-wave displacement of the main XEL peak, which is accompanied by its splitting into two narrow components peaked at λ_{m1} = 324 nm and at λ_{m2} = 305 nm (Fig. 3, curve 3). For the BaF_2 nanophosphor, already at 294 K, a long-wave component peaked at ~410 nm can be traced, although much less than that of CaF_2 nanophosphors [11]. Although for 294 K, the XEL light outputs in the single BaF_2 crystal and in nanoparticles are commensurable, the cooling of nanoparticles down to 80 K leads to a sharp increase in the intensity of the XEL peak (nearly 2.5 times) (Fig. 3, curve 4). Spectral displacement of the XEL peaks during the cooling of the nanophosphor down to 80 K is small (λ_{m1} = 321 nm, λ_{m2} = 305 nm). The intensity of the emission in the additional long wave band also significantly increases during the cooling of the nanophosphor down to 80 K.

Thus, the transition from the single BaF_2 crystal to similar nanoparticles is accompanied by a certain increase in the concentration of radiation defects during stationary X-irradiation, especially at low temperatures, and by a corresponding decrease in the radiation resistance of the nanophosphors, though to a much lesser extent than for the CaF_2 nanophosphors.

The change in the structure of the exciton emission spectra in the BaF_2 nanophosphors compared with the corresponding spectra of a single crystal can be explained by the action of the surface of nanoparticles on the energy structure of the excitons localized on the surfaces of the nanophosphor grains. This interpretation is confirmed by the deterioration of the separation of this peak in a coarse-grained sample for d = 113 nm (Figs. 4 and 5, curves 5), where the role of surface effects decreases in comparison with volumetric effects.

The dependence of the light output on the size of nanoparticles in the XEL spectra of the BaF_2 nanophosphors at the temperature of 80 K can be seen in Fig. 4.

The smallest light output is characteristic of the BaF_2 nanophosphors with the grain size of d = 20 nm (Fig. 4, curve 1), whose XEL spectrum forms a broad and weakly separated band peaked at nearly 382 nm. An increase in the size of nanoparticles up to d = 32 nm is accompanied by an extension of the XEL band and by some increase in its intensity (Fig. 4, curve 2).

The next increase in the grain size of BaF_2 nanophosphors up to d = 54 nm (Fig. 4, curve 3) and up to d = 78 nm (Fig. 4, curve 4) causes a significant increase in the emission intensity.

Starting with the size of the nanoparticles d = 54 nm, in the XEL spectra of BaF_2 there dominates the STE emission peak at 321 nm and a peak close to it at 305 nm. No peaks of this kind in fine-grained nanophosphors (with d = 20 nm and d = 32 nm) may be explained by a low probability of the formation of STE from them due to a too large, compared to the size of nanoparticles, mean free path of the primary photoelectrons during the creation of secondary electronic excitations within the matrix, that include, in particular, STE [2,3].

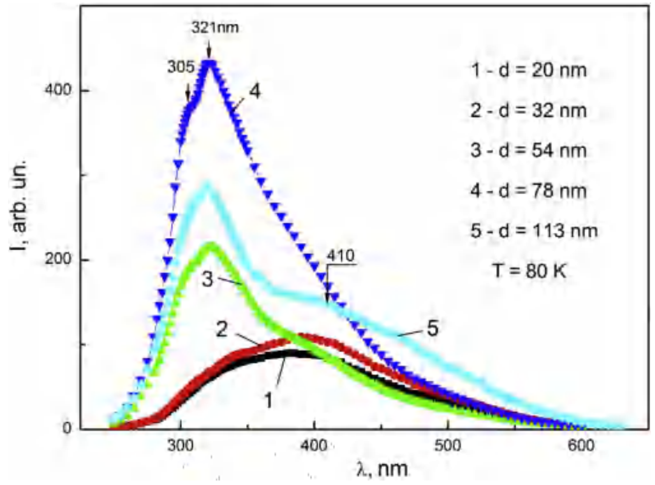

Fig. 4. X-ray excited luminescence spectra of the BaF_2 nanoparticles with different grain sizes d at the temperature of 80 K: 1–non-annealed, d = 20 nm, 2–d = 32 nm, 3–d = 54 nm, 4–d = 78 nm, 5–d = 113 nm.

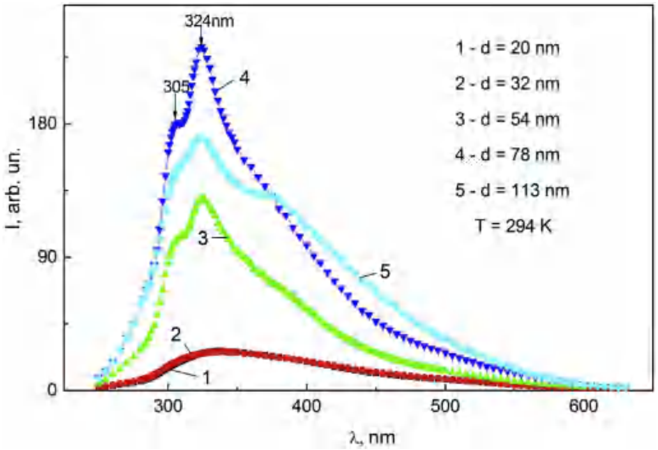

Fig. 5. X-ray excited luminescence spectra of the BaF_2 nanoparticles with different grain sizes d at the temperature of 294 K: 1–non-annealed, d = 20 nm, 2–d = 32 nm, 3–d = 54 nm, 4–d = 78 nm, 5–d = 113 nm.

The subsequent increase in the size of BaF_2 nanoparticles to d = 113 nm, on the contrary, leads to a decrease in the XEL light output (Fig. 4, curve 5). A similar decrease in the light emission in coarse-grained samples was observed even for the CaF_2 nanoparticles [11]. In our opinion, this occurs due to the peculiarities of the preparation of nanoparticles with d = 113 nm. The replacement of fluorine ions by oxygen ions during high-temperature annealing under normal atmospheric conditions may be one of the reasons for the drop in the intensity of luminescence. Another reason for the decrease in the intensity of emission may be the phenomenon of aggregation of nanophosphor grains at an increasing temperature of its annealing due to the rapid growth of the grain size, which is accompanied by an increase in a disordered crystalline structure. This, in turn, can lead to a non-emitting STE decomposition upon the lattice defects. This assumption is also supported by a certain increase in the relative intensity of the emission band at ~410 nm of the excitons localized on the lattice defects (Fig. 4, curve 5).

For 294 K, a decrease in the relative intensity of the longwave band of luminescence (~410 nm) can be observed for all grain sizes (Fig. 5).

This is evidently connected with the thermally activated decay of stable color centers in the BaF_2 matrix and with an increased probability of rapid recombination of electrons and holes formed in the process of the non-emitting decay of excitons. Thus, at room temperature, the radiation resistance of BaF_2 nanophosphors is greater than at 80 K.

At 294 K, the intensities of the XEL of BaF_2 nanophosphors with d = 20 nm and d = 32 nm are so close that their spectra nearly coincide (Fig. 5, curves 1 and 2). At 294 K, as well as at 80 K, the growth of the sizes of nanoparticles for d > ~80 nm leads to a significant decrease of the light output of stationary X-ray excited luminescence (Figs. 4 and 5, curve 5). Thus, with respect to the value of the XEL light output, the size of BaF_2 nanoparticles in the vicinity of 80 nm turns out to be optimal.

It is typical that the spectral separation of the peaks at 324 and 305 nm for 300 K deteriorates in nanoparticles of large sizes (d ≥ 113 nm) (Fig. 4 and 5, curve 5), which may be due to a decrease of the surface effect on the STE in large nanoparticles.

In our opinion, some of our research data provide an important indirect evidence that sample structure does not change during the increase of average particle sizes from 54 to 78 nm (agglomerates are not formed). This is evidenced by such experimental facts:

1) It is known that light output of self-trapped exciton luminescence, which is proportional to probability of their radiative decay, depends

on the crystal structure perfection and decreases with its violation when probability of non-radiative decay of excitons on lattice defects increases. Intensity of exciton luminescence in the peak region at ~320 nm of nanophosphors with grain diameter of 78 nm is close to the corresponding intensity for BaF$_2$ single crystal (Fig. 3), which gives evidence of low concentration of defects in these nanoparticles. Formation of nanoparticle agglomerates occurs only at annealing temperatures more than 800 C, when nanoparticle size exceeds 110 nm. This is accompanied by corresponding decrease in the luminescence light output of self-trapped excitons (Figs. 4 and 5, curves 5).

2) Relative intensity of emission band of excitons localized on lattice defects (assuming that they are anion vacancies) with peak at ~ 410 nm does not change in the 54–78 nm range of nanoparticle sizes, which also point to the absence of rapid growth of defects in nanoluminophores with corresponding grain sizes. Relative contribution of this band increases only for nanoparticles of 113 nm size, in which number of defects increases (Figs. 4 and 5, curves 5). Sharp increase in the intensity of emission band peaking at ~320 nm in the 54–78 nm range of nanoparticles is obviously due to coincident increase in probability of primary photoelectron interaction with nanoparticle lattice during formation of secondary electron excitations of the matrix, which include, in particular, STE.

3.2. Thermally stimulated luminescence of a single crystal and of the nanophosphors of BaF$_2$

Radiation defects that result in the appearance of a long-wavelength XEL band at ~410 nm in the single crystal and in nanophosphors of BaF$_2$ also cause the capture of charge carriers that occur in the samples when they are irradiated by X-ray at 80 K and before the appearance of thermally stimulated luminescence (TSL) at the subsequent heating of samples in the 80–300 K.

The whole TSL light output of BaF$_2$ single-crystal irradiated with X-ray at 80 K concentrates in two major peaks, close to the intensity located at 113 and 198 K, and in two weaker peaks: at 141 and 255 K (Fig. 6, curve 1). In the BaF$_2$ nanophosphor with the grain size of 78 nm, the TSL peaks are close to those in a single crystal, but these peaks differ much by the relative intensity: the TSL peak at 138 K is the main one in the nanophosphor while the peaks at 113 and 199 K are much weaker (Fig. 6, curve 2).

It has been previously established that the X-ray irradiation of BaF$_2$ crystals at 77 K leads to the formation of V_k- and F- coloring centers detected by the absorption bands, respectively, for 3.4 and 2.3 eV [7]. V_k- and F- centers are formed during the emissionless STE disintegration in BaF$_2$ crystals. At the same time, in the BaF$_2$ matrix, α- and I-centers can also be formed, specifically, anion vacancies and interstitial C1$^-$ ions, as well as H-centers, specifically, interstitial Cl^0 atoms.

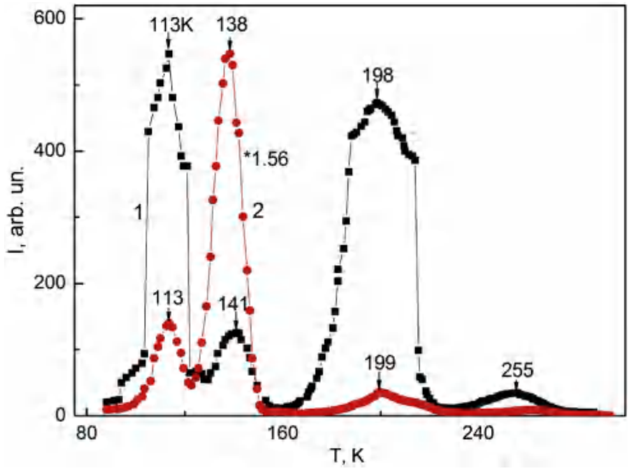

Fig. 6. Integral curves of thermostimulated luminescence of a single crystal (1) and the nanoparticles of BaF$_2$ with a grain size of 78 nm (2). The TSL in the T ≥ 240 K range for BaF$_2$ nanoparticles is hardly traceable.

It is known that the thermal delocalization of hole V_k-centers in the BaF$_2$ matrix takes place at a temperature of ~115 K [6]. Therefore, it is obvious that the TSL peak, which at 113 K can be traced both in the single crystal and in the BaF$_2$ nanophosphor, occurs during the delocalization of the V_k-centers and during their recombination with the electrons of the F-centers.

In the BaF$_2$ nanophosphor, the TSL peak at 113 K by its form (Fig. 6, curve 2) obviously belongs to the monomolecular recombination process (1- st order of kinetics), characterized by a steady increase and a sharp decrease of an intensity [14]. To determine the activation energy of V_k-centers, we used the appropriate Bichevin formula [15]:

$$E(eV) = 9.32\cdot10^{-5}T_m{}^2(1 + 1.26\,T_1/T_2)\cdot(T_2 - T_1)^{-1} \tag{1}$$

where T_m, T_1 and T_2 are the temperatures of the maximum and at the half-height of the TSL peak ($T_1 < T_2$). The corresponding activation energy of the V_k-centers E_{nph} (113 K) = 0.18 eV for the BaF$_2$ nanoparticles.

Unusual shape of the TSL peaks of BaF$_2$ single crystal (Fig. 6, curve 1) is due to their non-elementary nature. In particular, low-temperature peak at 113 K is a superposition of three elementary peaks: the main one is at 113 K, it corresponds to V_k-centers delocalization in BaF$_2$ matrix, and two peaks of lower intensity – at 108 and 120 K, associated with V_{kA}-centers delocalization, that are V_k-centers, localized in the vicinity of unidentified impurities. Since main contribution to this TSL peak is made by V$_k$-centers and taking into account the complex nature of the TSL peak, we used the Luschik formula [16] to determine the activation energy of V_k-centers in BaF$_2$ single crystal:

$$E(eV) = kT_m^2/(T_2 - T_m) \tag{2}$$

where k is Boltzmann's constant, T_m and T_2 are the temperatures of the maximum and at the half-height of the TSL peak ($T_m < T_2$). Corresponding activation energy of the V_k-centers E_{cr} (113 K) = 0.15 eV for BaF$_2$ single crystal. By the way, we got the same value for E_{cr} (113 K), and by formula (1). This indicates that in this case the linear nature of recombination kinetics of V_k-centers is dominant.

The second intensive TSL peak of the BaF$_2$ single crystal for 198 K (Fig. 6, curve 1) obviously corresponds to the delocalization of the H-centers and to their recombination with the electrons of the F- centers.

A similar TSL peak in CaF$_2$ nanophosphors is located at ~200 K [11], while in the isostructural SrCl$_2$ crystal, two similar peaks are observed: at 210 and at 227 K [10]. Activation energy of H-centers for BaF$_2$ single crystal, determined by formula (2): E_{cr} (198 K) = 0.24 eV.

In the BaF$_2$ nanophosphor, the corresponding TSL peak at 199 K is very weak (Fig. 6, curve 2), which indicatics a low probability of the formation of H-centers herein. This may be caused by the restriction, due to the nanoparticle size, of the d_{FH} distance between the F- and H-centers in the primary unstable F-H pair formed during the STE decomposition. It was shown earlier [6,17] that in crystals with a large d_{FH} distance, the best conditions are formed for the decomposition process of STE into the F-H pair.

The main TSL peak of BaF$_2$ nanophosphor with a grain size of 78 nm, located at 138 K (Fig. 6, curve 2), may appear due to the delocalization of the hole V_H-centers that occupy an intermediate position in the BaF$_2$ lattice by a symmetry between the V_k- and H-centers [11]. The monomolecular nature of the kinetics of the recombination process occurring at 138 K indicates that V_H- and F-centers form genetic pairs, that is, arise at the decay of the same self-locating exciton, and are located in close proximity to one another. This provides a high probability of (V_H-F)- recombinations The activation energy of V_H-centers in the BaF$_2$ nanophosphor, determined by formula (1), is E_{nph} (138 K) = 0.29 eV.

It turned out that the size of the nanoparticles strongly affects the amount of the TSL light output, which significantly increases in the

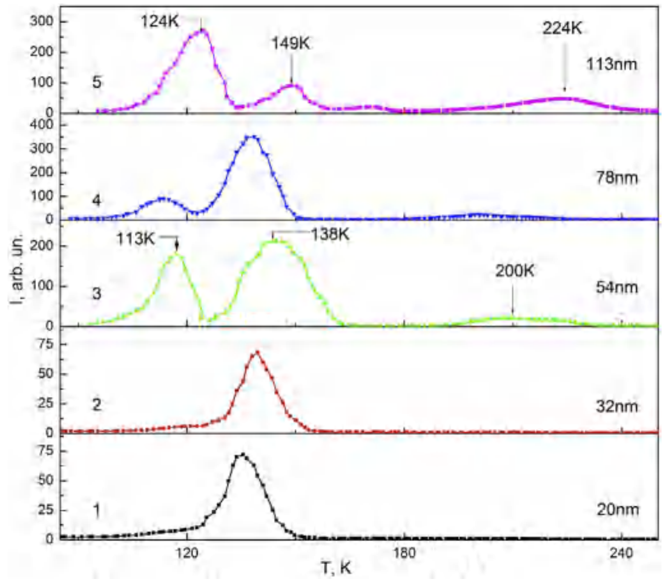

Fig. 7. Integral curves of thermostimulated luminescence of BaF_2 nanophosphors with different sizes of nanoparticles: 1–d = 20 nm, 2–d = 32 nm, 3–d = 54 nm, 4–d = 78 nm, 5–d = 113 nm irradiated by X-ray quanta at 80 K for 10 min.

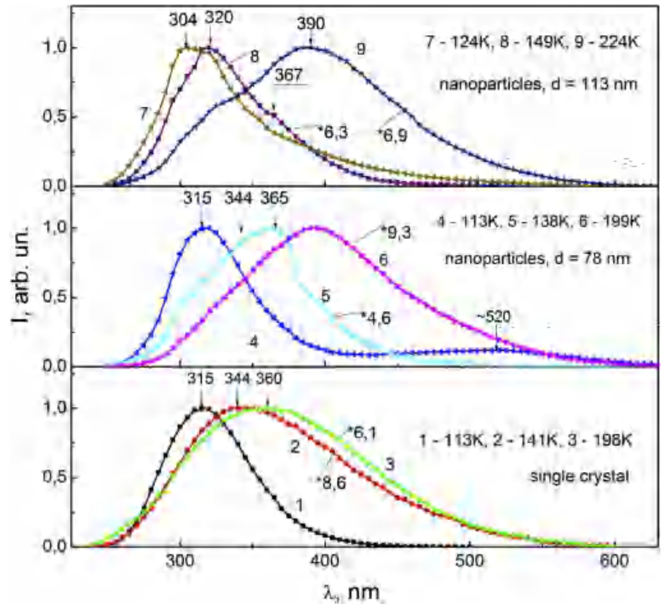

Fig. 8. Normalized spectra of thermostimulated luminescence of a single crystal (1, 2, 3) and nanophosphors of BaF_2 with different sizes of nanoparticles: d = 78 nm (4, 5, 6) and d = 113 nm (7, 8, 9) irradiated by X-ray quanta for 80 K for 10 min: 1, 4–T = 113 K, 2–T = 141 K, 3–198 K, 5–138 K, 6–199 K, 7–124 K, 8–149 K, 9–224 K.

range of 20–78 nm (Fig. 7, curves 1–4). However, the subsequent increase of the grain size up to 113 nm causes a significant decrease in the TSL light output (Fig. 7, curve 5), similar to the case of XEL.

Due to a low probability of the STE localization within the nanoparticles of small sizes (d = 20–32 nm) and, consequently, at a low probability of V_k-centers forming in them, the TSL peak at 113 K is not observed for these centers (Fig. 7, curves 1, 2 This peak occurs only for nanoparticles whose sizes are not less than 54 nm (Fig. 7, curves 3, 4). In nanoparticles of d = 113 nm, this peak shifts to T = 124 K (Fig. 7, curve 5), which corresponds to the localization of V_k-centers near unidentified lattice defects.

The normalized TSL spectra for the peak at 113 K of a single crystal and of the nanoparticles of BaF_2 for the size d = 78 nm are close to each other in the short-wave region (Fig. 8, curves 1 and 4) and contain the main band of 315 nm that coincides with the main XEL band of the BaF_2 single crystal at 80 K (Fig. 1, curve 2) associated with the STE emission.

Therefore, it is obvious that the recombination process of V_k-centers with electrons of the corresponding *F*-centers takes place by forming an STE with their typical emission band at 315 nm in the BaF_2 matrix. The absence of a fine structure in the TSL spectrum of the BaF_2 nanoparticles, which was traced in the spectra of their X-ray excited luminescence (Fig. 4, curves 3 and 4), is associated with a decrease in the measurement resolution of the TSL spectra due to doubling increase in the spectral width of the monochromator slot for the recording of the weak light fluxes of the TSL.

The TSL spectrum of the BaF_2 nanoparticles of size d = 78 nm for a peak at 113 K contains an additional weak band at ~520 nm, which may be due to the recombination of delocalized V_k centers with electrons captured by a cation sublattice, that is, with Ba^+ and Ba^0 centers. A similar band at 560 nm was detected in the XEL spectrum of CaF_2 nanoparticles [11].

For the nanoparticles of d = 113 nm size, the localization of the V_k-centers at the lattice defects leads not only to the displacement of the corresponding TSL peak to 124 K but also to a significant expansion and complication of the structure of the main band of its spectrum (Fig. 8, curve 7), where additional peaks at 304 and 320 nm are traced.

For the BaF_2 single crystal, the spectrum of TSL peak at 141 K, conventionally attributed to (V_H-*F*) recombinations, contains one broad band with the maximum at 344 nm (Fig. 8, curve 2). For the BaF_2 nanoparticles of the size d = 78 nm, a similar band of the TSL spectrum is traced for a peak at 138 K, where it expands and complicates by the structure (Fig. 8, curve 5). For BaF_2 nanoparticles of d = 113 nm size, the corresponding TSL spectrum at 149 K appreciably shifts to the short-wave side (up to 320 nm), but contains an additional weaker component at 367 nm.

For a single BaF_2 crystal, the TSL spectrum of the peak at 198 K, which was conventionally attributed to (*H-F*) recombinations, contains one broad band with a maximum at 360 nm (Fig. 8, curve 3). For BaF_2 nanoparticles of the sizes d = 78 nm and d = 113 nm, the maxima of the TSL spectra for respective peaks at 199 and 224 K appreciably shift in the longwave direction to ~390 nm (Fig. 8, curves 6 and 9), possibly due to spatial constraints of (*H-F*)- pairs in nanoparticles.

4. Conclusions

Essential differences were found in the spectra of stationary X-ray excited luminescence of BaF_2 nanophosphors at 294 and 80 K compared to the corresponding spectra of the BaF_2 single crystal. In BaF_2 nanophosphors at 294 K, there was detected an appreciable short-wave shift in the band of emission of self-trapped excitons (from 334 nm in a single crystal to ~ 320 nm in nanophosphors) and its significant narrowing and splitting into two components at 324 and 305 nm. The temperature drop to 80 K leads to an increase in the light output of the X-ray excited luminescence of BaF_2 nanophosphors by ~2.5 times, without significantly altering the spectral allocation of emission bands (at 321 and 305 nm). Such features in the emission spectra of X-ray excited luminescence of the BaF_2 nanophosphors can be explained by the action of the surface of nanoparticles on the energy structure of the excitons localized on the surfaces of the nanophosphor grains, as well as by the change in the character of the exciton-phonon interaction in comparison with the corresponding single crystal.

A slight decrease in the radiation resistance of the BaF_2 nanophosphors was observed compared to the corresponding single crystal, which led to an enhancement of an additional band at ~410 nm of X-ray excited luminescence that may be associated with the emission of the excitons localized in the vicinity of anionic vacancies of the matrix. At the same time, it was found that the radiation resistance of the BaF_2

nanophosphors is much higher compared to the CaF_2 nanophosphors, studied earlier [11].

By the changes of the integral TSL curves of the BaF_2 nanophosphors, compared to the corresponding curves of the BaF_2 single crystal, it was found that in the BaF_2 nanoparticles, the V_H-centers with a delocalization temperature at ~ 140 K are the preferred low-temperature hole coloring centers, in contrast to the BaF_2 single crystal with the dominating V_k- and H-centers. According to the TSL spectra, it was found that the placement of emission bands corresponding to the delocalization of V_k-centers in the nanoparticles and in the single-crystal of BaF_2 coincides with each other. At the same time, the spectral TSL bands due to (V_H-F)- and especially due to (H-F)- recombination in nanoparticles, are appreciably shifted to the long-wave side compared to the single crystal of BaF_2. These changes may also be due to the action of spatial constraints on effective distances in the genetic pairs of the hole and electron centers in the BaF_2 nanoparticles.

References

[1] Z. Luo, J.G. Moch, S.S. Johnson, C.C. Chen, Curr. Nanosci. 13 (2017) 364.
[2] V.V. Vistovskyy, A.V. Zhyshkovych, N.E. Mitina, A.S. Zaichenko, A.V. Gektin, A.N. Vasil'ev, A.S. Voloshinovskii, J. Appl. Phys. 112 (2012) 024325.
[3] V.V. Vistovskyy, A.V. Zhyshkovych, O.O. Halyatkin, N.E. Mitina, A.S. Zaichenko, P.A. Rodnyi, A.N. Vasil'ev, A.V. Gektin, A.S. Voloshinovskii, J. Appl. Phys. 116 (2014) 054308.
[4] R. Schmechel, H. Winkler, X. Li, M. Kennedy, M. Kolbe, A. Benker, M. Winterer, R.A. Fischer, H. Hahn, H. von Seggern, Scripta Mater. 44 (2001) 1213.
[5] C. Dujardin, D. Amans, A. Belsky, F. Chaput, G. Ledoux, A. Pillonnet, IEEE Trans. Nucl. Sci. 57 (2010) 1348.
[6] P.A. Rodnyi, Physical Processes in Inorganic Scintillators, CRC Press, Nev York, 1997.
[7] A.I. Nepomnyashchikh, E.A. Radzhabov, A.V. Egranov, V.F. Ivashechkin, A.S. Istomin, Radiat. Eff. Defect Solid 157 (2002) 715.
[8] E.P. Chinkov, S.A. Stepanov, V.F. Shtan'ko, T.S. Ivanova, IOP Conf. Ser. Mater. Sci. Eng. 110 (2016) 012050.
[9] V.M. Lisitsyn, L.A. Lisitsyna, A.I. Popov, E.A. Kotomin, F.U. Abuova, A. Akilbekov, J. Maier, Nucl. Instrum. Methods Phys. Res. B (2015), https://doi.org/10.1016/j.nimb.2015.08.002.
[10] O.T. Antonyak, YaM. Chornodolskyy, S.V. Syrotyuk, N.V. Gloskovska, R.V. Gamernyk, Mater. Res. Express 4 (2017) 116306.
[11] O.T. Antonyak, V.V. Vistovskyy, A.V. Zhyshkovych, I.M. Kravchuk, J. Lumin. 1w67 (2015) 249.
[12] YuM. Aleksandrov, V.N. Makhov, P.A. Rodnyi, T.I. Syreishchikova, M.N. Yakimenko, Sov. Phys. Solid State 26 (1984) 2865.
[13] J. Luo, S. Sahi, M. Groza, Z. Wang, L. Ma, W. Chen, A. Burger, R. Kenarangui, T.-K. Sham, F. Selim, Opt. Mater. 58 (2016) 353.
[14] K. Biswas, A.D. Sontakke, R. Sen, K. Annapurna, J. Fluoresc. 22 (2012) 745.
[15] V.V. Bichevin, Proc. Inst. Phys. Estonian Acad. of Sciences 52 (1981) 169.
[16] C. Furetta, Handbook of Thermoluminescence, World Scientific Publishing, Singapore, 2009.
[17] K.S. Song, C.H. Leung, R.T. Willams, J. Phys. Condens. Matter 1 (1989) 683.